Heliyon 10 (2024) e36118

Contents lists available at ScienceDirect

Heliyon

journal homepage: www.cell.com/heliyon

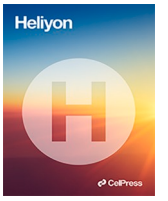

Research article

Wound healing potential of silver nanoparticles from *Hybanthus enneaspermus* on rats

Liang Cheng, Song Zhang, Qian Zhang, Wenjie Gao, Shengzhi Mu *, Benfeng Wang **

Department of Burns and Plastic Surgery, Shaanxi Provincial People's Hospital, Xi'an, 710068, China

ARTICLE INFO

Keywords:
Hydroxyproline
Excision wound
Silver nanoparticles
Hybanthus enneaspermus
RAW 264.7 cells

ABSTRACT

In this study, we green synthesized silver nanoparticles (Ag Nps) from *Hybanthus enneaspermus* leaves (HE-Ag NPs) and evaluated their antimicrobial and wound-healing properties. The synthesized HE-Ag NPs were characterized using various techniques, revealing face-centered polygonal structures, a well-dispersed appearance, and an average particle size of 42–51 nm. The antimicrobial effects of HE-Ag NPs and their embedded cotton fabrics were tested against several pathogens, showing effective inhibition of growth. The cytotoxicity and anti-inflammatory properties of HE-Ag NPs were assessed using MTT assays on L929 and RAW 264.7 cells and by measuring inflammatory cytokine levels in LPS-treated RAW 264.7 cells. HE-Ag NPs did not affect the viability of L929 and RAW 264.7 cells and significantly reduced inflammatory cytokine levels. *In vivo* studies using an excision wound model demonstrated that HE-Ag NPs-loaded ointment significantly increased hydroxyproline, total protein, and antioxidant levels and enhanced the wound contraction rate. These findings suggest that HE-Ag NPs have potent antimicrobial properties and promote wound healing, indicating their potential for use in topical ointments for wound care.

1. Introduction

The skin is the biggest organ of the connective tissue system and plays an important role in numerous bodily processes; it accounts for about 15 % of total body weight. The skin's fundamental role is to protect the body's internal organs and tissues from outside factors [1]. Due to this, the skin is the most vulnerable part of the body, and it can be easily injured by things like cuts and scrapes. Skin injuries can be caused by a variety of physical, biological, and chemical agents [2]. A wound is any disruption in the structure of the skin, whether from external factors like trauma or surgery or internal ones like disease. Damage might be minimal, affecting only the epithelial layers of the skin, or it can be severe, affecting not only the subcutaneous layer but also the underlying structures [3].

Acute and chronic wounds undergo a wound repair process that may be divided into four stages: homeostasis/coagulation, inflammation, proliferation, and maturation. Platelets and the initiation of the coagulation cascade play pivotal roles in the first stage. At this early stage, fibrin strands bind to the wound site, encouraging the development of a thrombus or clot and entrapping platelets in the injury site [4]. In the inflammatory stage, the wound site recruits inflammatory cells to clean up the injured cells and infections.

* Corresponding author.
** Co-corresponding author.
E-mail addresses: mszping@163.com (S. Mu), wbf123789@sina.com (B. Wang).

https://doi.org/10.1016/j.heliyon.2024.e36118
Received 26 January 2024; Received in revised form 8 August 2024; Accepted 9 August 2024
Available online 10 August 2024
2405-8440/© 2024 Published by Elsevier Ltd. This is an open access article under the CC BY-NC-ND license (http://creativecommons.org/licenses/by-nc-nd/4.0/).

However, wound healing is slowed by inflammation if the inflammatory phase lasts too long and an excessive number of activated cells are recruited to the wounded area [5].

A variety of factors can easily disrupt the wound-healing process, some of which may have detrimental effects on the healing process. Chronic wounds that fail to heal due to a variety of causes including infection, pollution, old age, diabetes, and the use of certain medications like corticosteroids [6]. These factors need to be taken into consideration and a proper treatment strategy established. Topical treatments comprise a major portion of wound healing agents, and their primary function is infection prevention rather than wound healing. Nanoparticles (NPs) have been synthesized for a variety of biological uses in recent decades because of their unique physiochemical characteristics compared to those of traditional materials. In general, metallic NPs have several advantages, including controllable optical characteristics, corrosion resistance, and recyclability [7]. As a result, research into nanoparticles as potential antimicrobial alternatives is proceeding rapidly. Silver nanoparticles (AgNPs) are the most effective antibacterial nanoparticles [8].

Due to its proven antibacterial and wound-healing capabilities, nano-silver has remarkable potential in therapeutic applications, even among other metallic NPs including gold, copper, iron, titanium, and zinc [9]. This is due to their potency as an antibacterial even at low concentrations, as well as their ease of synthesis and immobilization on fabrics. The concentration of silver nanoparticles (AgNPs) needed to be effective antimicrobials is substantially lower than the lowest amount considered acceptable for human exposure. The constant release of Ag + ions from silver nanoparticles is responsible for their antibacterial activity [10]. This disrupts the bacterial membrane and electron transport. Likewise, DNA gets damaged by the Ag + ions. AgNPs exhibit absorption at UV wavelengths; hence, AgNP-treated textiles also protect against UV radiation [11]. Antimicrobial textiles have seen an upsurge in demand in recent years due to rising consumer hygiene requirements. Commercially available antimicrobial textiles have been around for years, but the rise of drug-resistant microbes that are unaffected by antibiotics has sparked interest in treating textiles with nanoparticles that exhibit broad-spectrum antimicrobial activity [12].

Patients who have used topical steroids for a long time and suddenly stop using them may experience symptoms known as topical steroid withdrawal (TSW), which has recently drawn attention to topical therapies and led to some controversy. The redness, burning, and itching are all signs of this condition [13]. Therefore, effective alternatives to commercial wound-healing medications are urgently needed. Synthesizing NPs from natural materials like plants has gained a lot of attention as a low-cost, easy, rapid, and scalable alternative to traditional synthetic methods [14]. Since they are rich in bioactive composites that are amenable to performing the roles of reducing and doping agents, the biocompatibility of these natural products is a significant advantage [15–17].

Plants have been used medicinally for thousands of years due to their bioactive compounds, which protect against chronic diseases, reduce oxidative stress, and improve lipid profiles, blood pressure, and gastrointestinal health [18]. *H. enneaspermus* (Violaceae family) is an herb or shrub that grows in all regions of tropical countries worldwide. It was already mentioned that the roots are widely utilized to treat various conditions, including urinary tract infections, gonorrhea, and cholera, and also have tonic, diuretic, demulcent, and aphrodisiac properties [18]. Furthermore, this plant has been highlighted to demonstrate anti-oxidant [19], anti-diabetic [20], anti-arthritic [21], anti-bacterial [22], aphrodisiac [23], nephroprotective [24], and anti-inflammatory [25,26] properties. In the current work, we aim to synthesize the silver nanoparticles from the *H. enneaspermus* plant embedded in the cotton textiles and evaluate their anti-microbial and excision wound healing properties.

2. Materials and methods

2.1. Chemicals

The silver nitrate ($AgNO_3$), microbial growth media, and other chemicals were attained from Sigma-Aldrich, USA. To measure the biochemical markers, the corresponding kits were procured from eBioscience, USA.

2.2. Collection of plant sample

The fresh and insect-bite-free leaves of *H. enneaspermus* were collected from a local commercial vendor. The leaves were washed with water, dehydrated in the shade, and powdered using a mechanical grinder. The fine powder of the leaves was employed to extract the preparation and synthesize Ag NPs.

2.3. Preparation of H. enneaspermus leaf aqueous extract

The 50 g of leaf powder was added to 200 mL of deionized water and heated on a heating plate at 90 °C for 30 min to obtain the aqueous extract. The resulting crude plant extract was utilized to synthesize the Ag NPs after being cooled to 37 °C and filtered using Whatman No. 1 paper.

2.4. Synthesis of Ag NPs from H. enneaspermus

The 10 mL of *H. enneaspermus* extract was added to the 90 mL of AgNO3 (1 mM) in a 250 mL flask and kept at 37 °C in a dark place to synthesize Ag NPs. At intervals of every 30 min, the color transformation from clear to brown was checked. The suspension after the color change was centrifuged at 15,000 rpm for 30 min. The pellet was then resuspended in distilled water after the supernatant was removed. The resulting Ag NPs were then used for the characterization studies.

2.4.1. Characterization of the synthesized HE-Ag NPs

The study used UV–visible spectroscopic techniques to study the development of HE-Ag NPs in suspension (UV–visible spectrophotometer; Shimadzu-1700, Japan). The absorbance of the HE-Ag NPs was determined at various wavelengths between 200 and 800 nm, and their stretching and bonding were studied using FT-IR. Spectra were taken at 4500-500 cm^{-1} on a KBr disc with a Shimadzu-8400S spectrometer. The crystallinity of the developed HE-Ag NPs was studied using an X-ray diffractometer (X'pert Pro PANalytical System). The size and dispersion of the synthesized HE-Ag NPs were studied using TEM analysis (TECNAI F30, USA). The sample HE-Ag NPs were dispersed on a copper grid and illuminated under electronic radiation.

2.4.2. Coating of HE-Ag NPs on the cotton fabrics

The pure cotton fabric was purchased from a textile market. Then, after 1 h of soaking in boiling water (50 mL) with non-ionic detergent (2 mL/L), it is rinsed with water to remove the dirt and dust from the textile.

The study involved introducing sterile cotton fabrics with *H. enneaspermus* leaf extract, containing Ag NPs, through ultrasonication. The textiles were then washed, dehydrated, and cut into cube shapes for further examination. The HE-Ag NPs-embedded cotton fabrics were used for characterization and anti-microbial assessment against various pathogens. The resulting textiles were then used for further examinations and further research.

2.4.3. Scanning electron microscope (SEM) and energy dispersive X-ray (EDAX) analysis of the HE-Ag NPs-embedded cotton fabrics

SEM with EDAX spectroscopy was utilized to study the morphology and elemental compositions of the HE-Ag NP-embedded cotton fabrics. The JEOL/EO JSM-5600 SEM analyzer (JEOL, Japan) was used for the SEM and EDAX analyses.

2.5. Anti-microbial study

The synthesized HE-Ag NPs and their embedded cotton fabrics were tested for their anti-microbial efficacy against bacteria that cause skin infections. After inoculating the pure culture of each pathogen, wells were punched out to a size of 6 mm. After 24 h at 35 °C, each well was loaded with the HE-Ag NPs (20, 40, and 60 μg) and embedded cotton fabrics HE-Ag NPs were placed on the plates, respectively. Finally, the plates were investigated to observe for inhibitory zones.

2.6. Biological studies

2.6.1. In vitro cytotoxicity assay

The MTT assay was employed to determine the effect of synthesized HE-Ag NPs on the growth of non-malignant fibroblast L929 cells and macrophage-like RAW 264.7 cells. Briefly, various concentrations of HE-Ag NPs (2.5, 5, 7.5, 10, 12.5, and 15 μg) were added to the L929 and RAW 264.7 cell lines. After 24 h of incubation in DMEM media with HE-Ag NPs loaded cells, the cells were analyzed. The 10 μl of MTT reagent was mixed into each well for 2 h and then the formed formazan depositions were cleared by the addition of DMSO, and absorbance was taken at 570 nm.

2.6.2. Analysis of inflammatory cytokine levels in the RAW 264.7 cells

The RAW 264.7 cells were challenged with 200 ng/mL of lipopolysaccharide (LPS) and treated with the 7.5 and 10 μg of synthesized HE-Ag NPs for 24 h. Then, the control and treated cells were employed to prepare the homogenates using the cell lysis buffer. The prepared cell homogenates were utilized to examine pro-inflammatory cytokines such as IL-6, IL-8, IL-1β, and TNF-α levels using the respective kits following the protocols provided by the kit's manufacturer (eBioscience, USA).

2.7. Experimental in vivo animal study

In this study, male Wistar rats weighing 180–220 g were used, and they were caged in sterile polypropylene cabins with a temperature of 24 ± 3 °C, humidity of 55.4 %, and a 12 h dark/light cycle.

2.7.1. Formulation of HE-Ag NPs loaded topical ointment

A simple ointment was prepared by using a specific procedure, as described by the British Pharmacopoeia [27]. The melted paraffin (0.5 g) was added to a mixing bowl, followed by cetostearyl alcohol (0.5 g), wool fat (0.5 g), and yellow soft paraffin (8.5 g). The mixture was decanted to discard the contaminants and then agitated continuously until it reached room temperature. Finally, the synthesized HE-Ag NPs (100 mg/kg) were added to the basic ointment base at a 1 % concentration.

2.7.2. Excision wound model and treatment procedure

The study involved surgically wounding acclimated animals using an excision wound model under anesthesia. The animals were anesthetized with ketamine and diazepam before the injury. A circular excision wound was created, and the rats were divided into three groups: Group I Control (untreated), Group II Treatment (1 % of HE-Ag NPs-loaded ointment), and Group III positive control (5 % w/w povidone-iodine ointment). The rate of wound closure was observed on the 0^{th}, 7th, 14th, and 21st days post-wound, with day 0 being considered a day of wound development.

2.7.3. Measurement of wound contraction rate

The wound contraction rate was measured using the below formula, which uses the initial wound size of 314 mm2 as 100 %. The time to epithelization was calculated by observing when the dead tissue completely covered the wound without showing signs of a raw wound.

Wound closure (%) = wound area (day 0) – wound area (day of observation)/wound area (day 0) X 100.

2.7.4. Measurement of hydroxyproline content

The wound tissues from the experimental rats were excised on the final day of the study and subjected to estimation of hydroxyproline and total protein contents. The level of hydroxyproline was measured [28] using the assay kit as per the instructions given by the kit's manufacturer (Elabscience, USA). The total protein content was measured using the Lowry et al. [29] technique.

2.7.5. Analysis of oxidative stress and antioxidant markers

The oxidative and anti-oxidative biomarkers such as malondialdehyde (MDA), SOD, CAT, GPx, and GSH in the excised wound tissues of the experimental rats were analyzed using the assay kits by the techniques suggested using the kit's manufacturer (Bioscience, USA).

2.7.6. Histopathological analysis

The experiment involved excising wound skin tissues for histological analysis. The tissues were cut at 7 μm thickness, stained with hematoxylin and eosin, fixed in formalin, and embedded in paraffin wax. Sections were evaluated for fibroblast proliferation, collagen production, angiogenesis, and epithelialization by an independent panel.

2.8. Statistical analysis

One-way ANOVA and Tukey's post hoc assay were performed to examine the results, and each data was given as a mean ± SD of triplicates. The statistical variations were fixed significant for $p < 0.05$.

3. Results

3.1. Characterization of the synthesized PK-Ag NPs

The results of the UV-spectral analysis are shown in Fig. 1A. The development of Plant extract and HE-Ag NPs in the reaction medium was confirmed by the absorbance spectrum. The spectrum was measured between 200 and 800 nm wavelengths. The

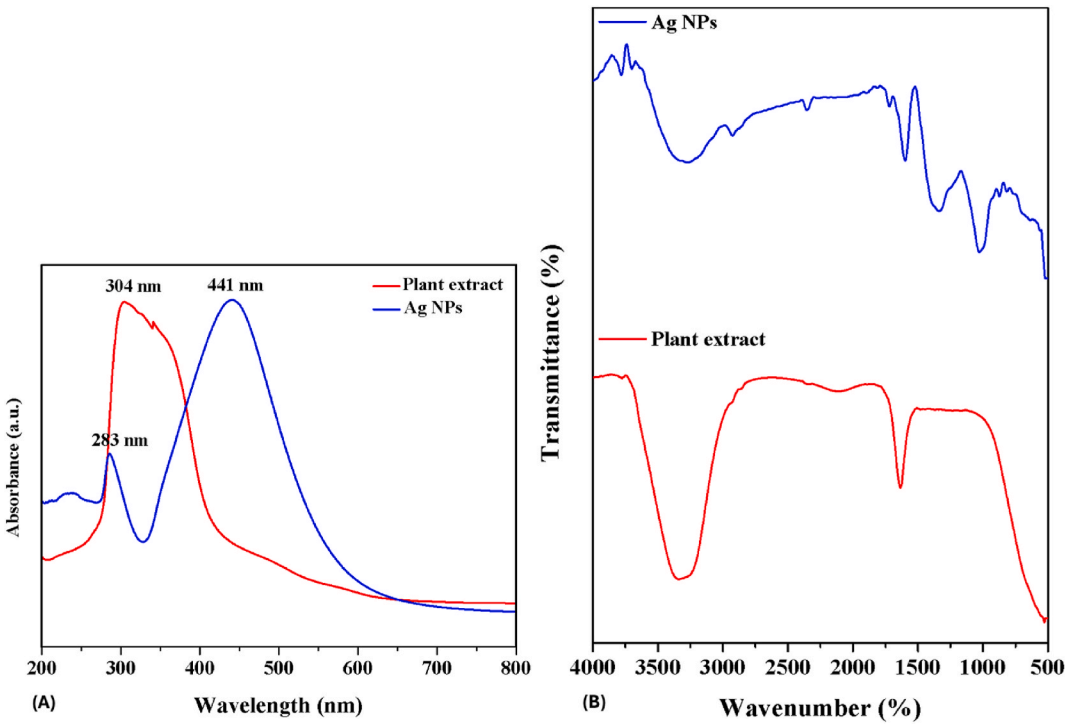

Fig. 1. (A) UV–visible spectroscopy and (B) FT-IR analysis of the HE-Ag NPs.

absorbance edge peaks were observed at 304 nm (283 nm and 441 nm) for plant extract and HE-Ag NPs, respectively.

Fig. 1B reveals the findings of the FT-IR study, which demonstrate the presence of various functional groups in the plant extract and synthesized HE-Ag NPs. The HE plant extract showed functional groups at 3324, 2102, 1632, and 533 cm^{-1}, corresponding to O–H stretching, aliphatic C–H stretching, and C–O stretching vibrations of flavonoids/phenolic groups. The HE-Ag NPs revealed several peaks at different frequencies in the spectrum, notably at 3781, 3698, 3279, 2931, 2862, 1714, 1611, 1017, and 525 cm^{-1}. The hydroxyl O–H stretching peaks were observed at 3781, 3698, and 3279 cm^{-1}. The C–H asymmetric and symmetric groups were observed at 2931 and 2862 cm^{-1}. The carboxylic group C=O peaks were found at 1714 and 1611 cm^{-1}. The C–O–C and secondary O–H groups were observed at 1017 cm^{-1}, and the metal Ag peak was 525 cm^{-1}.

The crystallinity of the synthesized HE-Ag NPs was investigated using XRD analysis (Fig. 2A). The XRD diffraction 2theta angle at 38.00°, 44.17°, 64.35°, and 77.33°, which correspond to the hkl planes of (111), (200), (220), and (311), respectively, for face-centered cubic phase characteristic of Ag structure (JCPDS no: 89–3722) and an average crystalline size of 37.81 nm, as evidenced by the occurrence of various peaks. The shape, size, and distribution patterns of the HE-Ag NPs were studied using TEM analysis (Fig. 2B). The TEM images revealed cubic, polygonal-shaped HE-Ag NPs with an average particle size of 42–51 nm.

The appearance of the HE-Ag NPs embedded on the cotton fabrics was investigated using SEM along with EDAX, and the findings are depicted in Fig. 3. The SEM microphotographs of the HE-Ag NPs-embedded cotton fabrics indicate the formation of dispersed HE-Ag NPs and their occurrence on the cotton fabrics (Fig. 3A). The findings of the EDAX study of HE-AgNPs-coated cotton fabrics revealed a higher percentage of Ag ions (Fig. 3B, C & D). These findings confirmed the development of HE-Ag NPs, their binding, and their existence on the surface of cotton fabrics.

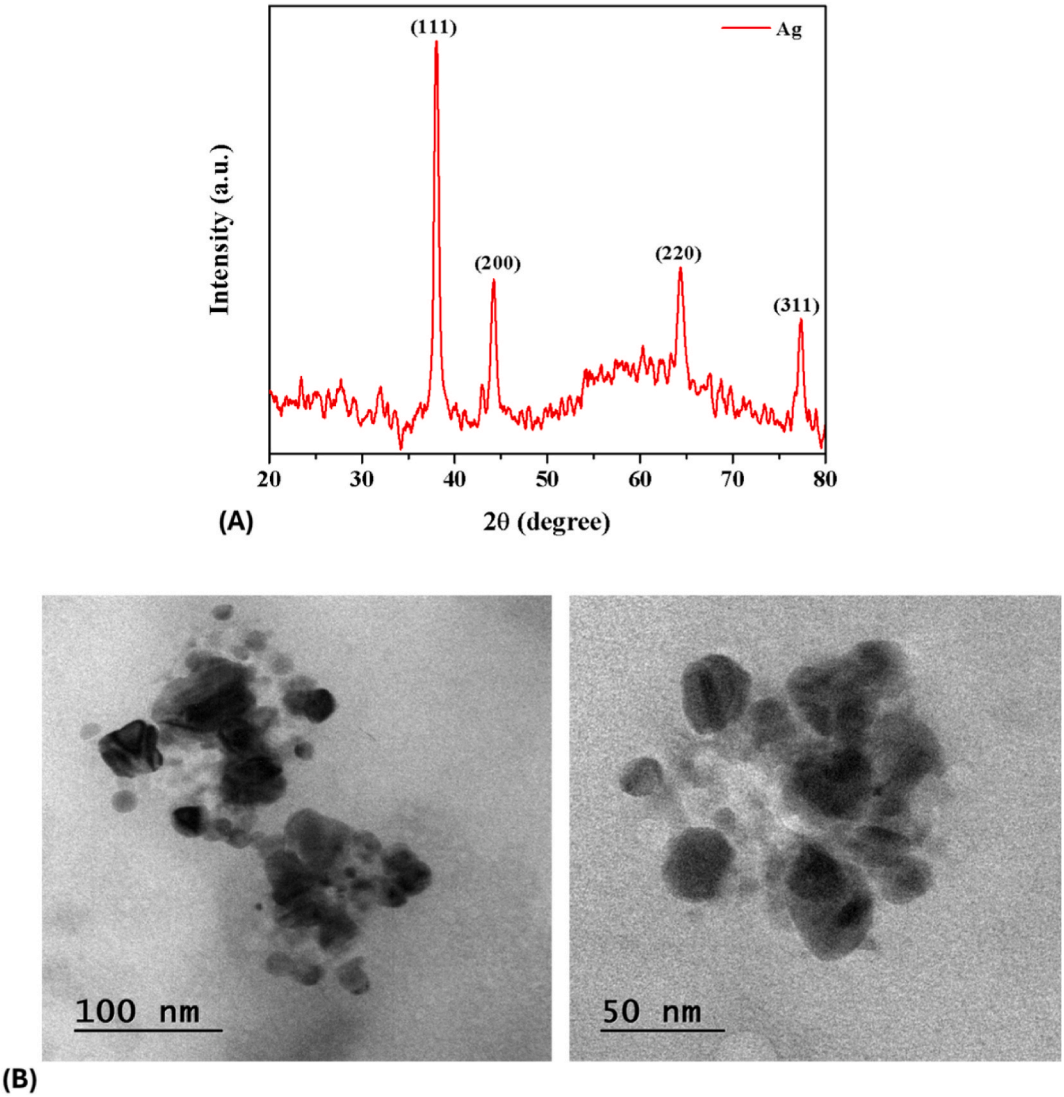

Fig. 2. (A) XRD and (B) TEM analysis of the HE-Ag NPs.

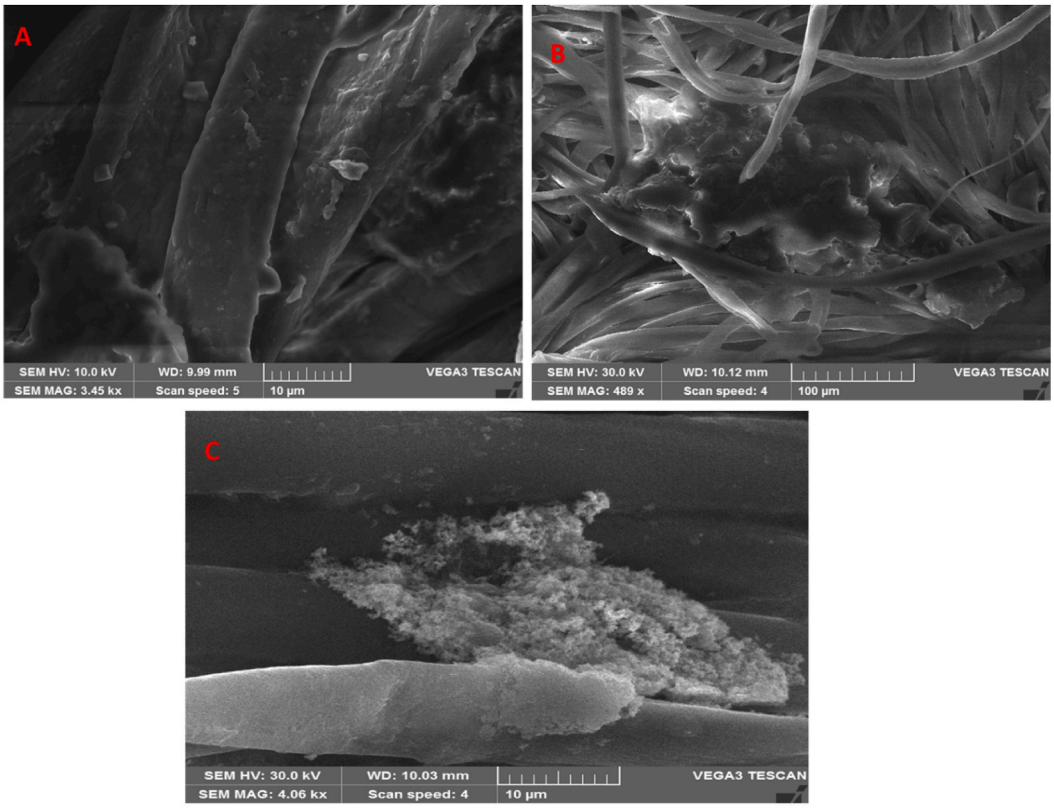

Element	Weight %	Atomic %	Net Int.	Error %	Kratio	Z	R	A	F
AgL	100.00	100.00	1081.34	1.60	1.0000	1.0000	1.0000	1.0000	1.0000

Fig. 3. (A, B & C) SEM and EDAX (D) analysis of the HE-Ag NPs-embedded cotton fabrics. The appearance of the HE-Ag NPs embedded in the cotton fabrics was investigated using SEM along with EDAX. The SEM images indicated the formation of dispersed HE-Ag NPs and their occurrence on the cotton fabrics (A, B & C). The EDAX analysis revealed that HE-Ag-coated cotton fabrics have the highest Ag ions (D).

3.2. Anti-microbial effect of the synthesized HE-Ag NPs

The anti-microbial effects of the HE-Ag NPs were tested against several pathogens, including *P. aeruginosa*, *K. pneumoniae*, *E. coli*, and *S. aureus*. The results proved that the HE-Ag NPs-loaded wells demonstrated increased inhibition zones around the well, which confirms that the HE-Ag NPs effectively inhibited microbial growth. The maximum inhibition zones were observed in *K. pneumoniae* (19 mm) and *P. aeruginosa* (18 mm) against 60 μg of HE-Ag NPs (Table 1). Overall, the NPs treatment considerably inhibited the growth of all the tested pathogens (Fig. 4).

3.3. Antimicrobial effect of HE-Ag NPs-embedded cotton fabrics

The cotton fabrics, which are coated with HE-Ag NPs were tested for their anti-microbial properties against various pathogens (Fig. 5). As indicated in Table 2, the treatment with the HE-Ag NPs-embedded cotton fabrics effectively inhibited the microbial growth. The maximum inhibitory zones were observed against *K. pneumoniae* (20 mm) and *P. aeruginosa* (19 mm). These findings indicated that the HE-Ag NPs-embedded cotton fabrics considerably inhibited the growth of several pathogens.

3.4. In vitro studies

3.4.1. Effect of synthesized HE-Ag NPs on the viability of L929 and RAW 264.7 cells

The viability of HE-Ag NPs-treated L929 and RAW 264.7 cells was measured using the MTT assay, and the findings are revealed in Fig. 6. The outcomes proved that the treatment of HE-Ag NPs at various concentrations did not disturb the growth of both L929 and RAW 264.7 cells. The growth of both cells remained unchanged up to the tested concentrations of the HE-Ag NPs. These findings evidence that HE-Ag NPs are non-toxic to normal cells.

3.4.2. Effect of HE-Ag NPs on the levels of pro-inflammatory cytokines in the LPS-induced RAW 264.7 cells

Fig. 7 represents the IL-6, IL-1β, IL-8, and TNF-α levels in the control and treated RAW 264.7 cells. The LPS-treated cells revealed increased levels of cytokines than the control. Interestingly, the treatment with 7.5 and 10 μg of HE-Ag NPs considerably diminished these cytokines in the LPS-induced cells.

3.5. In vivo studies

3.5.1. Effect of HE-Ag NPs on the total protein and hydroxyproline levels

The levels of total protein and hydroxyproline were measured in the wound tissues of the placebo and HE-Ag NP-treated rats. The levels of both total protein and hydroxyproline were significantly low in the wound tissues of the placebo control. However, the treatment with the HE-Ag NPs-loaded ointment considerably elevated both protein and hydroxyproline in the wound tissues of the rats (Fig. 8). A considerable increase in these markers was also noted in the standard drug povidone-iodine-treated rats, which supports the results of the HE-Ag NPs treatment.

3.5.2. Effect of HE-Ag NPs on the oxidative stress parameters

Fig. 9 demonstrates the results of oxidative and antioxidative parameter levels on the wound tissues of placebo and HE-Ag NP-treated rats. The wound tissues of the placebo rats had a significantly increased MDA level while having reduced CAT, SOD, GPx, and GSH levels. Whereas the topical administration of HE-Ag NPs-loaded ointment effectively boosted the antioxidant levels while decreasing the MDA level. Similar results were also observed on the standard drug povidone iodine ointment treatment, which corroborates the findings of the HE-Ag NPs.

3.5.3. Effect of HE-Ag NPs on the in vivo wound healing

The wound contraction rate was determined in the placebo and HE-Ag NPs-treated experimental rats (Fig. 10). The proportion of wound contraction rate significantly increased in the rats treated with HE-Ag NPs-loaded ointment. On the 0^{th}, 7th, 14th, and 21st days of observation, the NPs demonstrated a considerably higher wound closure rate than the placebo. The standard drug povidone-iodine treatment also considerably increased the wound closure rate (Fig. 11).

Table 1
Antibacterial activity of the synthesized HE-Ag NPs. The synthesized HE-Ag NPs at various concentrations (20, 40, and 60 μg) considerably inhibited the pathogen's growth. The highest inhibition zone was noted in *K. pneumoniae* (19 mm) and *P. aeruginosa* (18 mm) against 60 μg of synthesized HE-Ag NPs.

S.NO	Name of the organisms	20 μg	40 μg	60 μg	Negative control
01	*Escherichia coli*	12 mm	13 mm	14 mm	No Zone
02	*Klebsiella pneumoniae*	17 mm	18 mm	19 mm	No Zone
03	*Pseudomonas aeruginosa*	16 mm	17 mm	18 mm	No Zone
04	*Staphylococcus aureus*	15 mm	16 mm	17 mm	No Zone

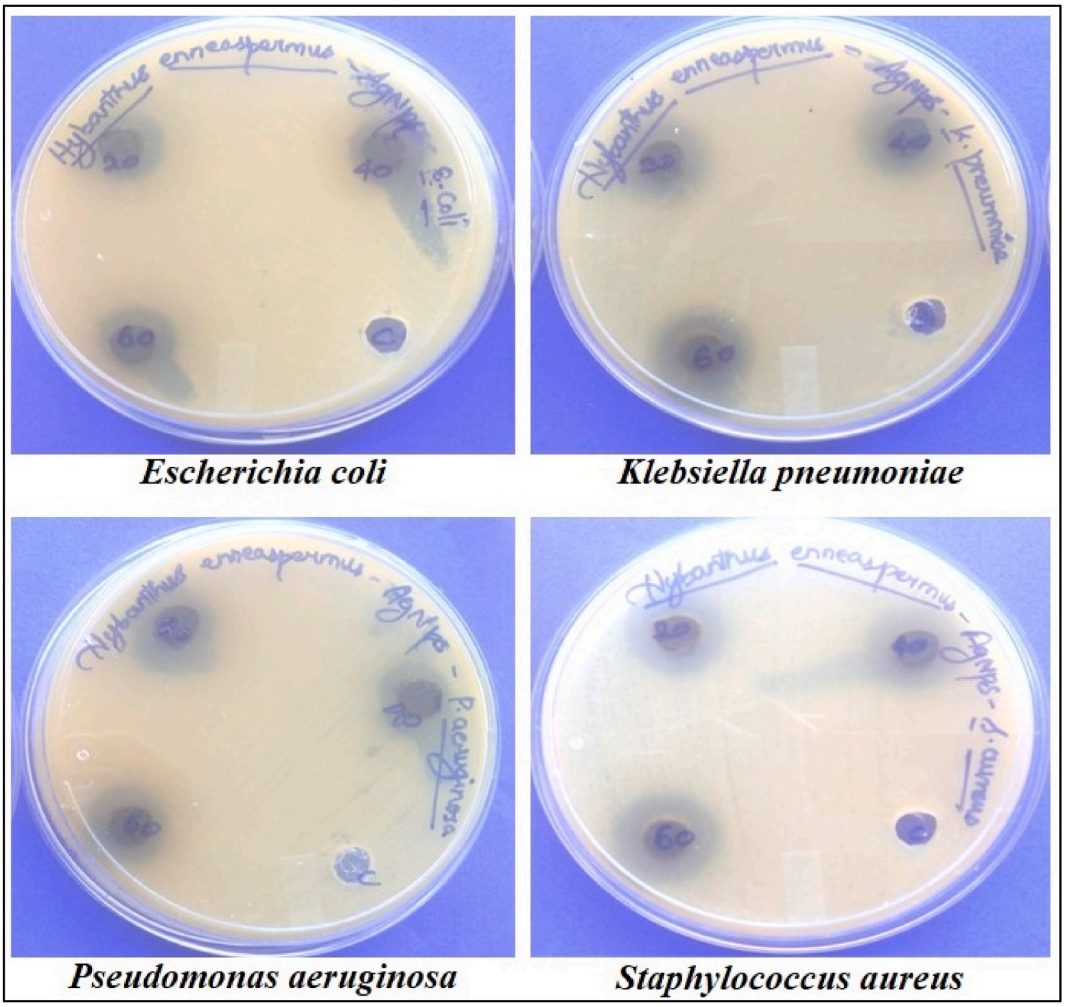

Fig. 4. Anti-bacterial activity of the HE-Ag NPs. The synthesized HE-Ag NPs at various concentrations (20, 40, and 60 μg) considerably inhibited the pathogen's growth. The highest inhibition zone was noted on the *K. pneumoniae* and *P. aeruginosa* against 60 μg of synthesized HE-Ag NPs.

3.5.4. Effect of HE-Ag NPs on the wound histopathology

The histopathology of wound tissues was analyzed, and the outcomes were revealed in Fig. 12. The untreated rats showed considerable changes such as fibrosis, infiltration of inflammatory cells, epithelium degradation, and inflammation. However, the wound tissues of the HE-Ag NPs-loaded ointment-treated rats had well-organized collagen fiber development, a thick epidermal layer, and reduced inflammatory cell infiltration. The tissues of HE-AgNPs-loaded ointment-treated rats had no symptoms of inflammation in the regenerated tissues. Similar results were also noted in the wound tissues of the povidone-iodine-treated rats, which supports the activity of HE-Ag NPs.

4. Discussion

Skin wounds are a primary interest for the public health sector due to their prevalence and negative impacts on patient wellbeing. Hospitalization and antibiotics may be necessary if the wound does not heal quickly enough or if a pathogen infection occurs [30]. Topical treatments that speed up wound healing are a promising area of research. Wound healing is a dynamic, self-sustaining process that is impacted by various factors, including cytokines, blood, extracellular matrix, and growth hormones. Bleeding control and infection prevention are the cornerstones of wound care. It has been shown that using active substances with antioxidant, antibacterial, anti-inflammatory, and cell proliferation properties is the most effective method for treating wounds [31]. Therefore, the current work was focused on analyzing the beneficial properties of synthesized HE-Ag NPs in terms of their anti-microbial, anti-inflammatory, proliferative, antioxidant, and *in vivo* wound healing activities.

Numerous bacterial infections can prolong the healing process by keeping wounds infected for longer. Any topical treatment for a wound needs to be effective against bacteria and other microorganisms. When compared to other types of microbes, such as fungi, bacteria are the most frequently isolated from wounds. The skin acts as a protective layer against the colonization of harmful

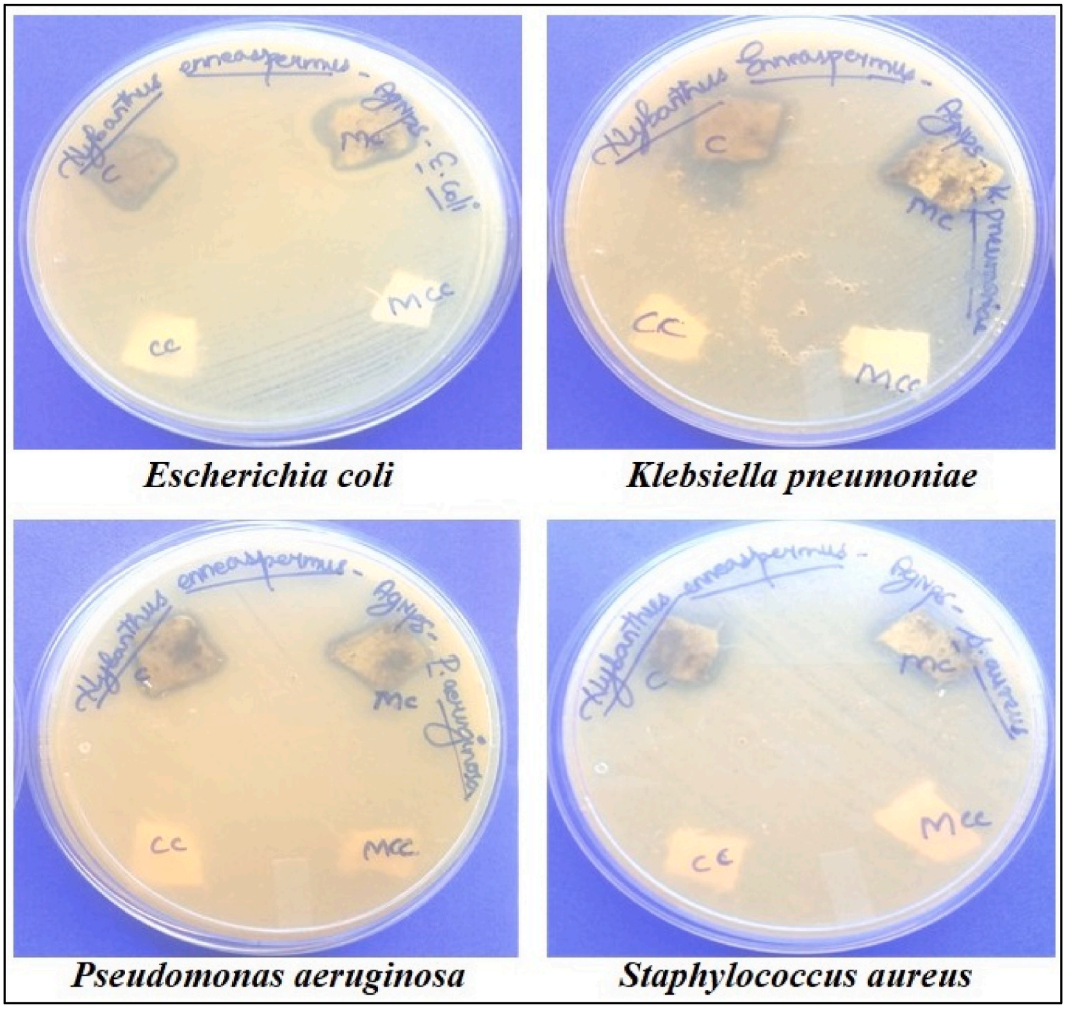

Fig. 5. Anti-bacterial activity of the HE-Ag NPs-coated cotton fabrics. The cotton fabrics, which are coated with HE-Ag NPs revealed considerable anti-microbial effects against the tested pathogens. Control (C), Mixed cotton (MC), Cotton control (CC), and Mixed cotton control (MCC). The maximum inhibition was observed against *K. pneumoniae* and *P. aeruginosa*.

Table 2
Antibacterial activity of the synthesized HE-Ag NPs-coated cotton fabrics. The cotton fabrics, which are coated with HE-Ag NPs, demonstrated antimicrobial effects against the tested pathogens. The maximum inhibition was noted against *K. pneumoniae* (20 mm) and *P. aeruginosa* (19 mm).

S.NO	Name of the organisms	Cotton	Mixed cotton	Cotton control	Mixed cotton control
01	*Escherichia coli*	17 mm	18 mm	No Zone	No Zone
02	*Klebsiella pneumoniae*	19 mm	20 mm	No Zone	No Zone
03	*Pseudomonas aeruginosa*	18 mm	19 mm	No Zone	No Zone
04	*Staphylococcus aureus*	17 mm	18 mm	No Zone	No Zone

microorganisms, but when it is damaged, the underlying tissue is exposed to infection [32]. The damaged skin allows bacteria to enter the wound, where they can then spread and eventually colonize the area. The mere existence of such nonreplicating microorganisms represents contamination. Microorganisms can get colonized after being introduced through contamination, and this process can continue without triggering an immune response [33].

To effectively deal with multi-drug-resistant bacterial strains, it is crucial to find a new method for researching novel antibiotic agents. It is well known that metal NPs, especially silver, are applied to cuts, burns, and wounds to prevent infection because they act as antibacterial agents and may control a wide range of microorganisms [34]. Most of the commercial wound healing agents used presently fail to provide satisfactory results. Nanotechnology is a reliable research topic for wound-healing drugs because of its many unique physiochemical properties. Silver has long been utilized in traditional medicines and food products due to its propensity to be sterile. Ag NPs have been the subject of a plethora of research due to their potential antibacterial effects [35]. The current results

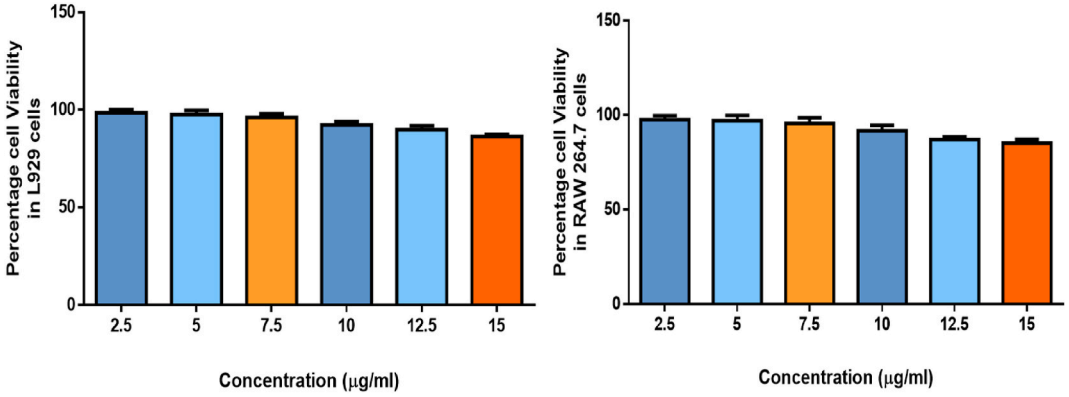

Fig. 6. Effect of HE-Ag NPs on the viability of L929 and RAW 264.7 cells. Results were taken from triplicate assays and given as a mean ± SD of triplicates. The values are analyzed using the one-way ANOVA and Tukey's post hoc assay.

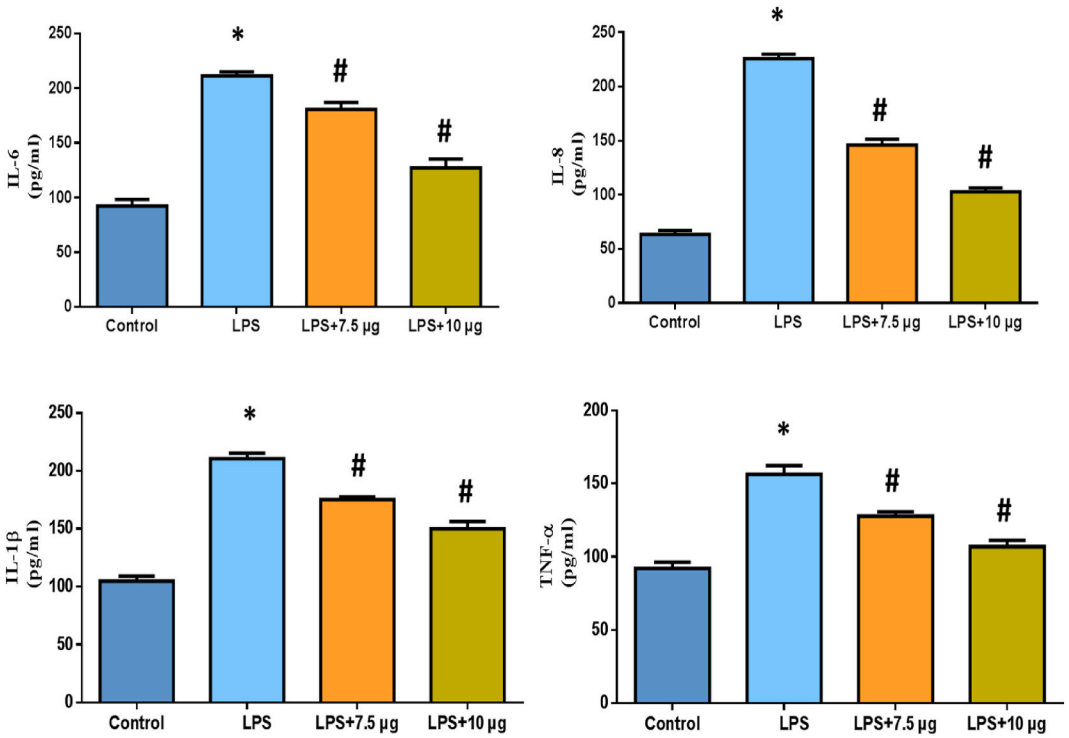

Fig. 7. Effect of HE-Ag NPs on the levels of pro-inflammatory cytokines in the LPS-induced RAW 264.7 cells. Results were obtained from triplicate assays and given as a mean ± SD of triplicates. The values are analyzed using the one-way ANOVA and Tukey's post hoc assay. Note: '*' represents that data are significant at $p < 0.05$ from the control and '#' represents that the data are significant at $p < 0.01$ from the LPS-induced group.

proved that both synthesized HE-AgNPs and their embedded cotton fabrics effectively inhibited the growth of the tested pathogens, i.e., *P. aeruginosa, K. pneumoniae, E. coli, and S. aureus*. These findings indicated that the HE-Ag NPs and coated cotton fabrics are effective against pathogens due to their strong anti-microbial properties.

The primary role of the proliferative phase in wound healing is to cover and fill the wound. At these points, active and differentiated fibroblasts, known as myofibroblasts, start contracting the wound margins. After that, re-epithelialization begins, which is triggered by the deposition of extracellular matrix, primarily collagen [36]. Finally, during the maturation phase of healing, collagen fibers are rearranged and the tissue is reformed to become stiff and flexible [37]. In this work, the influence of HE-Ag NPs was investigated on the proliferation of normal skin fibroblast L929 cells as well as macrophage-like RAW 264.7 cells. These outcomes highlight that the HE-Ag NPs treatment effectively increased the growth of L929 as well as RAW 264.7 cells. Therefore, it is clear that the HE-Ag NPs can promote the wound healing process by promoting the fibroblast proliferation rate.

Previous studies have explored the biosynthesis of Ag nanoparticles using *Heracleum persicum* seeds' methanolic extract, which

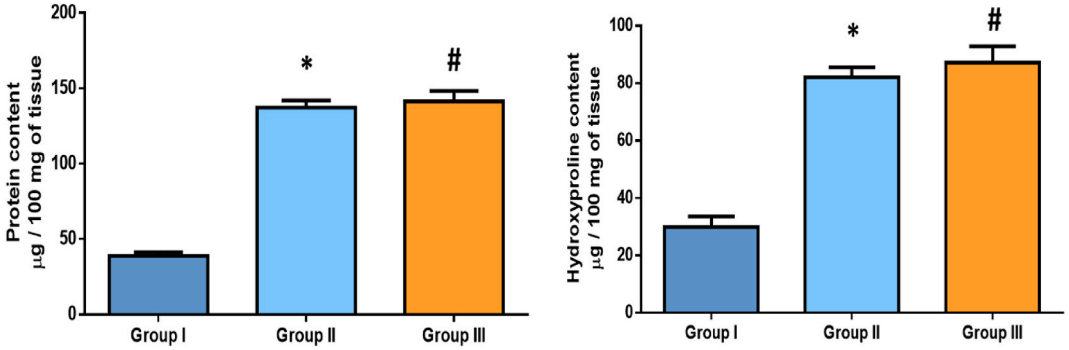

Fig. 8. Effect of HE-Ag NPs on the total protein and hydroxyproline levels (µg/100 mg of tissue) in wound tissues of the placebo. Values are expressed as mean ± SD for experiments. The values are analyzed using the one-way ANOVA and Tukey's post hoc assay. Note: '*' represents that data are significant at $p < 0.05$ from group I and '#' represents that the data are significant at $p < 0.01$ from LPS-induced group II.

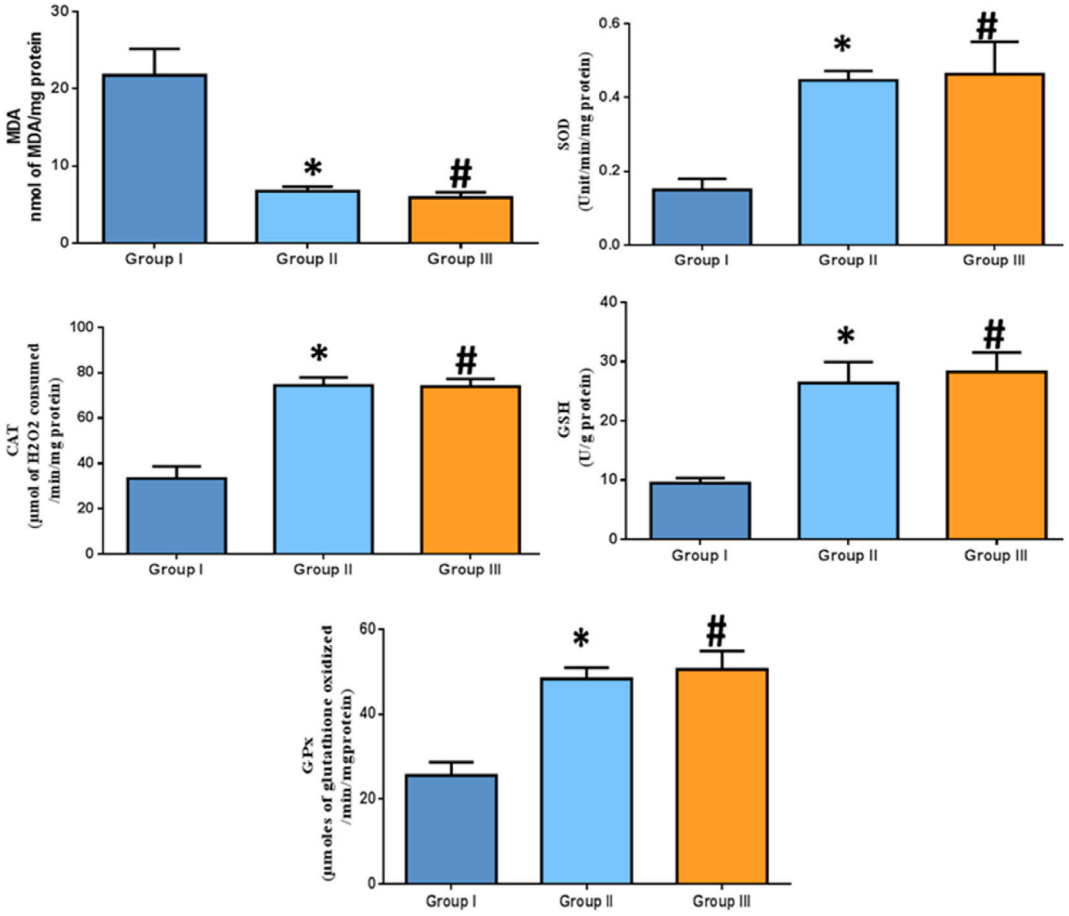

Fig. 9. Effect of HE-Ag NPs on the oxidative and anti-oxidative parameter levels. Results were obtained from expressed as mean ± SD for experiments. The values are analyzed using the one-way ANOVA and Tukey's post hoc assay. Note: '*' represents that data are significant at $p < 0.05$ from group I and '#' represents that the data are significant at $p < 0.01$ from LPS-induced group II.

showed a decrease in livability against human breast adenocarcinoma cell lines. This suggests that Ag NPs could be a green drug for treating breast adenocarcinoma [38]. An eco-friendly method for synthesizing copper nanoparticles (CuNPs) from *Thymus fedtschenkoi* leaves extract showed growth-inhibiting effects on lung cancer cell lines [39]. A modern drug containing iron nanoparticles (FeNPs) containing *Glycyrrhiza glabra* L leaf for treating acute lymphoblastic leukemia showed low cell viability against MOLT-3, CEM/C2, TALL-104, and CCRF-CEM cell lines, with the best cytotoxicity observed in the CCRF-CEM cell line [40].

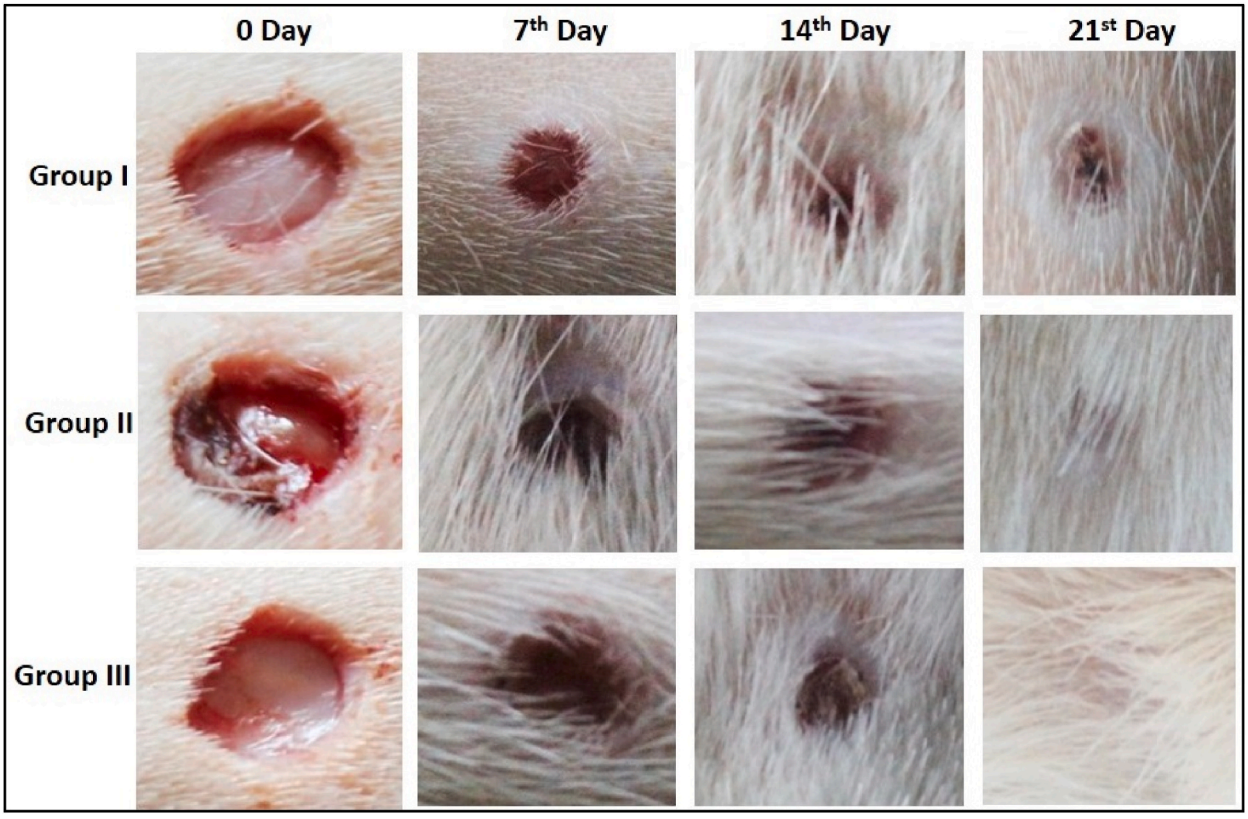

Fig. 10. Effect of HE-Ag NPs on the *in vivo* wound healing activity. The topical administration of ointment with HE-Ag NPs increased the wound contraction rate in rats with excision wounds. Group I: Control, Group II: HE-Ag NPs-loaded ointment, and Group III: Standard drug.

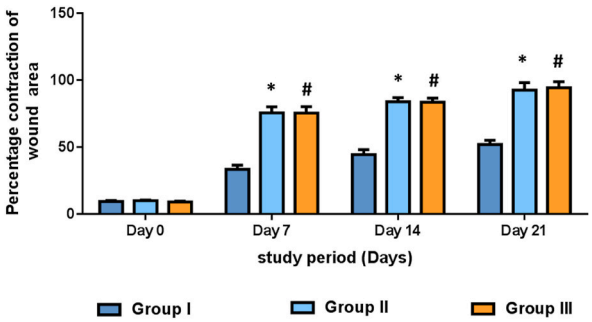

Fig. 11. Effect of HE-Ag NPs on the *in vivo* wound contraction rate. Results were obtained as a mean ± SD. The values are analyzed using the one-way ANOVA and Tukey's post hoc assay. Note: '*' represents that data are significant at $p < 0.05$ from group I and '#' represents that the data are significant at $p < 0.01$ from LPS-induced group II.

Previous studies have discovered the therapeutic properties of copper nanoparticles with antioxidant potential for treating infectious diseases and cutaneous wounds [41]. A new series of 18 thiosemicarbazones (TSCs) was synthesized and tested against various enzymes using the Forcefield Method [42]. A chemotherapeutic drug using *Rhus coriaria* L. fruit aqueous extract showed significant anticancer effects against human Caucasian carcinoma [43]. Lens culinaris seed extract conjugated gold nanoparticles may be a potential dietary therapeutic agent for treating acute myeloid leukemia due to their antioxidant properties and potential chemotherapeutic benefits [44]. The study suggests that *Camellia sinensis* leaf extract-based gold nanoparticles may be a potential dietary therapeutic for treating acute myeloid leukemia, with similar antioxidant properties to doxorubicin [45].

Chronic inflammation can hinder the wound healing mechanism and result in the formation of chronic wounds [46], so it's important to mitigate inflammation as much as possible. Pro-inflammatory cytokines are crucial in the early stages of wound healing [47]. At the wound site, monocytes undergo a process of terminal differentiation into macrophages, during which they release several cytokines like IL-1β, IL-6, and TNF-α [48]. TNF-α is responsible for the organization of collagen fibers and the suppression of tissue

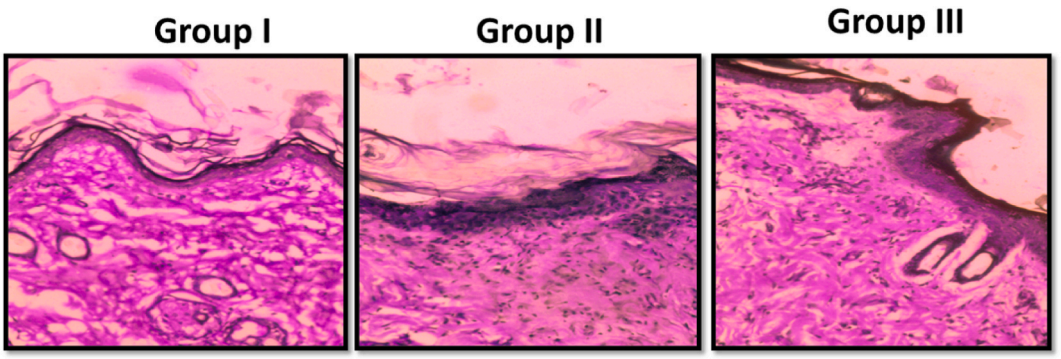

Fig. 12. Effect of HE-Ag NPs on wound histopathology. The untreated rats showed considerable changes such as fibrosis, infiltration of inflammatory cells, and inflammation (Group I). The wound tissues of the HE-Ag NPs-loaded ointment-treated rats had well-organized collagen fiber, reduced inflammatory cell infiltration, and no symptoms of inflammation in the regenerated tissues (Group II). Similar results were also noted on the wound tissues of the povidone iodine-treated rats (Group III).

granulation. Increased development of granulation tissue, which is full of cells and capillaries, is necessary for the remodeling phase of healing [49]. Diller et al. [50] highlighted that the expression of genes encoding anti-inflammatory markers is down-regulated, whereas pro-inflammatory cytokines and chemokines are elevated during the inflammatory phase. It has been found that the addition of anti-inflammatory medications to wounds might be beneficial, as they can reduce inflammation for longer and help the wound transition from the inflammatory to the healing phase [51]. This is because fibroblast and keratinocyte proliferation and migration are slowed by chronic inflammation, which in turn slows the process of re-epithelization [52]. Therefore, in this study, we analyzed the impacts of HE-Ag NPs on the inflammatory cytokine levels in LPS-challenged RAW 264.7 cells. The findings proved that the HE-Ag NPs treatment considerably reduced the secretion of IL-1β, IL-6, IL-8, and TNF-α, which proved their anti-inflammatory properties. Therefore, it was clear that the HE-Ag NPs can aid in the wound healing process by mitigating the inflammatory response.

Hydroxyproline, the main amino acid in collagen, is used as a biomarker for the presence of collagen in tissue samples. Higher levels of hydroxyproline indicate an increase in collagen production, which in turn improves wound healing. Collagen seems to play a pivotal role in the growth of healing tissues; both lysine and proline hydroxylation are required for collagen production [53]. In addition, the presence of more hydroxyproline indicates that the wound is closing more rapidly. Increases in electrostatic and ionic interactions between collagen molecules are reflected in a higher hexosamine concentration. Collagen is essential for homeostasis and epithelialization, two processes that occur during the last phases of wound healing and are necessary to maintain the strength and integrity of the tissue matrix. Repaired tissue and the overall healing pattern are consequently boosted by increased hydroxyproline production [54]. In the current investigation, an increased amount of hydroxyproline, as well as total protein, was found by biochemical examination of the wound tissues from HE-Ag NPs-loaded ointment-treated rats, suggesting an increase in collagen synthesis and cellular proliferation. These findings proved that the HE-Ag NPs can promote wound healing by up-regulating hydroxyproline secretion.

When skin is damaged, it releases an inflow of free radicals and oxidants into the surrounding area. Due to the high production of ROS during oxidative metabolism involving unpaired electrons, oxidative stress slows wound healing and increases cytotoxicity in biological systems. The healing of wounds is aided by antioxidants because they lessen the wound's exposure to oxidative stress [55–57]. A vital enzyme known as SOD neutralizes the more dangerous superoxide radical by converting it to the less hazardous hydrogen peroxide. CAT defends cells from damage caused by a wide range of harmful substances. CAT eliminates H2O2 and breaks it down into water and oxygen. This is the first line of defense against oxygen radicals. Cells are detoxicated when GPx and GSH function together, and H2O2 is eliminated by GSH oxidation [58]. Reduced oxidative stress has been linked to increased antioxidant activity at the wound site [59]. Since eliminating free radicals is a key step in wound healing, it is essential to measure antioxidant molecules including CAT, SOD, and MDA [60]. The current results showed that treatment with an ointment containing HE-Ag NPs increased the levels of CAT, SOD, GPx, and GSH while decreasing the amount of MDA in the wound tissues. These findings prove that HE-Ag NPs can increase wound healing by mitigating oxidative stress and boosting antioxidants in the wound tissues.

Wound healing is the process of restoring injured tissue to a state as similar to its original condition as possible by reconstructing its cellular structures and tissue layers. The fibroblastic stage of healing is the beginning of a mechanism called wound contracture, which results in wound closure. Epithelization, angiogenesis, and collagen deposition are all hallmarks of the proliferative phase [61]. In this work, the outcomes of *in vivo* wound healing exhibited that the topical administration of HE-Ag NPs-loaded ointment considerably increased the wound contraction rate. The findings of histological analysis also revealed that the wound tissues of the HE-Ag NPs-loaded ointment-treated rats had well-organized collagen fibers, a thick epidermal layer, reduced inflammatory cell infiltration, and signs of inflammation. These results proved that the HE-Ag NPs effectively supported wound healing in the rat excision wound model.

5. Conclusions

This study found that silver nanoparticles from *H. enneaspermus* leaves (HE-Ag NPs) can significantly improve wound healing in a

rat model. The ointment accelerated the healing process, reducing oxidative stress and promoting tissue regeneration. *In vitro* experiments confirmed the nanoparticles' anti-inflammatory properties, reducing inflammation in macrophage cells. The study also confirmed the antimicrobial efficacy of HE-Ag NPs and HE-Ag NPs-embedded cotton fabrics against pathogenic microorganisms. These findings suggest HE-Ag NPs have the potential for advanced wound care treatments. When HE-Ag NPs-containing ointment was applied to the wound, the healing process significantly increased by mitigating oxidative stress and increasing hydroxyproline levels. The findings of *in vitro* experiments proved that the HE-Ag NPs increased the growth of L929 and reduced the inflammatory cytokines in the LPS-induced RAW 264.7 cells. It was also shown that the HE-Ag NPs and their embedded cotton fabrics were effective against various pathogens. The wound-healing potential of HE-Ag NPs suggests that they could be used as a potent wound-healing agent.

Funding statement

This work was supported by Natural Science Basic Research Program of Shaanxi (Grant No. 2023-JC-QN-0874) and Industry-University-Research Innovation Fund of Science and Technology Development Center of Ministry of Education (Grant No. 2021JH044).

Data availability

Data will be made available on request.

Ethical approval

Shaanxi Provincial People's Hospital, Approval Number.2022k059.

CRediT authorship contribution statement

Liang Cheng: Writing – review & editing, Methodology, Investigation. **Song Zhang:** Investigation, Data curation. **Qian Zhang:** Supervision, Investigation, Conceptualization. **Wenjie Gao:** Investigation, Data curation, Conceptualization. **Shengzhi Mu:** Writing – review & editing, Software, Resources. **Benfeng Wang:** Writing – original draft, Methodology, Investigation.

Declaration of competing interest

The authors declare that there are no conflicts of interest.

References

[1] E. Christophers, J.M. Schröder, Evolution of innate defense in human skin, Exp. Dermatol. 31 (2022) 304–311, https://doi.org/10.1111/exd.14482.
[2] K. Varaprasad, T. Jayaramudu, V. Kanikireddy, C. Toro, E.R. Sadiku, Alginate-based composite materials for wound dressing application: a mini-review, Carbohydr. Polym. 236 (2020) 116025, https://doi.org/10.1016/j.carbpol.2020.116025.
[3] Y. J Son, W.T. John, Y. Zhou, W. Mao, E.K. Yim, H.S. Yoo, Biomaterials and controlled release strategy for epithelial wound healing, Biomater. Sci. 7 (2019) 4444–4471, https://doi.org/10.1039/C9BM00456D.
[4] D.R. Childs, A.S. Murthy, Overview of wound healing and management, Surgical Clinics. 97 (2017) 189–207, https://doi.org/10.1016/j.suc.2016.08.013.
[5] S.K. Dev, P.K. Choudhury, R. Srivastava, M. Sharma, Antimicrobial, anti-inflammatory and wound healing activity of polyherbal formulation, Biomed. Pharmacother. 111 (2019) 555–567, https://doi.org/10.1016/j.biopha.2018.12.075.
[6] P.G. Rodriguez, F.N. Felix, D.T. Woodley, E.K. Shim, The role of oxygen in wound healing: a review of the literature, Dermatol. Surg. 34 (2008) 1159–1169, https://doi.org/10.1111/j.1524-4725.2008.34254.x.
[7] L. Wang, M.H. Kafshgari, M. Meunier, Optical properties and applications of plasmonic-metal nanoparticles, Adv. Funct. Mater. 30 (2020) 2005400, https://doi.org/10.1002/adfm.202005400.
[8] B. Chen, F. Li, X.K. Zhu, W. Xie, X. Hu, M.H. Zan, X. Li, Q.Y. Li, S.S. Guo, X.Z. Zhao, Y.A. Jiang, Highly biocompatible and recyclable biomimetic nanoparticles for antibiotic-resistant bacteria infection, Biomater. Sci. 9 (2021) 826–834, https://doi.org/10.1039/D0BM01397H.
[9] P. Balashanmugam, H.J. Kim, V. Singh, R.S. Kumaran, Green synthesis of silver nanoparticles using Ginkgo biloba and their bactericidal and larvicidal effects, Nanosci. Nanotechnol. Lett. 10 (2018) 422–428, https://doi.org/10.1166/nnl.2018.2630.
[10] A.I. Ribeiro, D. Senturk, K.K. Silva, M. Modic, U. Cvelbar, G. Dinescu, B. Mitu, A. Nikiforov, C. Leys, I. Kuchakova, M. De Vrieze, Antimicrobial efficacy of low concentration PVP-silver nanoparticles deposited on DBD plasma-treated polyamide 6, 6 fabric, Coatings 9 (2019) 581, https://doi.org/10.3390/coatings9090581.
[11] S. Arora, N. Tyagi, A. Bhardwaj, L. Rusu, R. Palanki, K. Vig, S.R. Singh, A.P. Singh, S. Palanki, M.E. Miller, J.E. Carter, Silver nanoparticles protect human keratinocytes against UVB radiation-induced DNA damage and apoptosis: potential for prevention of skin carcinogenesis, Nanomed. Nanotechnol. Biol. Med. 11 (2015) 1265–1275, https://doi.org/10.1016/j.nano.2015.02.024.
[12] T. Gulzar, T. Farooq, S. Kiran, I. Ahmad, A. Hameed, The Impact and Prospects of Green Chemistry for Textile Technology, 2019, pp. 1–20.
[13] T. Hajar, Y.A. Leshem, J.M. Hanifin, S.T. Nedorost, P.A. Lio, A.S. Paller, J. Block, E.L. Simpson, A systematic review of topical corticosteroid withdrawal ("steroid addiction") in patients with atopic dermatitis and other dermatoses, J. Am. Acad. Dermatol. 72 (2015) 541–549, https://doi.org/10.1016/j.jaad.2014.11.024.
[14] F. Ahmad, N. Ashraf, T. Ashraf, R.B. Zhou, D.D. Yin, Biological synthesis of metallic nanoparticles (MNPs) by plants and microbes: their cellular uptake, biocompatibility, and biomedical applications, Appl. Microbiol. Biotechnol. 103 (2019) 2913–2935, https://doi.org/10.1007/s00253-019-09675-5.
[15] Y.Y. Loo, Y. Rukayadi, M.A. Nor-Khaizura, C.H. Kuan, B.W. Chieng, M. Nishibuchi, S. Radu, In vitro antimicrobial activity of green synthesized silver nanoparticles against selected gram-negative foodborne pathogens, Front. Microbiol. 9 (2018) 1555, https://doi.org/10.3389/fmicb.2018.01555.
[16] M.G. Arafa, R.F. El-Kased, M.M. Elmazar, Thermoresponsive gels containing gold nanoparticles as smart antibacterial and wound healing agents, Sci. Rep. 8 (2018) 13674.
[17] H. Huang, X. Qi, Y. Chen, Z. Wu, Thermo-sensitive hydrogels for delivering biotherapeutic molecules: a review, Saudi Pharmaceut. J. 27 (2019) 990–999, https://doi.org/10.1016/j.jsps.2019.08.001.

[18] M. Samtiya, R.E. Aluko, T. Dhewa, J.M. Moreno-Rojas, Potential health benefits of plant food-derived bioactive components: an overview, Foods 10 (4) (2021) 839, https://doi.org/10.3390/foods10040839.
[19] K.R. Retnam, A. Britto, Pharmacognostical Study of Hybanthus Enneaspermus (Linn.) F. Muell, 2007.
[20] D.A. Priya, S. Ranganayaki, P.S. Devi, Phytochemical screening and antioxidant potential of Hybanthus enneaspermus: a rare ethano botanical herb, J. Pharm. Res. 4 (2011) 1497–1502.
[21] D.K. Patel, R. Kumar, S.K. Prasad, K. Sairam, S. Hemalatha, Antidiabetic and in vitro antioxidant potential of Hybanthus enneaspermus (Linn) F. Muell in streptozotocin-induced diabetic rats, Asian Pac. J. Trop. Biomed. 1 (2011) 316–322, https://doi.org/10.1016/S2221-1691(11)60051-8.
[22] S. Tripathy, S.P. Sahoo, D. Pradhan, S. Sahoo, D.K. Satapathy, Evaluation of anti-arthritic potential of Hybanthus enneaspermus, African Journal of Pharmacy and Pharmacology 3 (2009) 611–614.
[23] S. Sahoo, D.M. Kar, S. Mohapatra, S.P. Rout, S. K Dash, Antibacterial activity of Hybanthus enneaspermus against selected urinary tract pathogens, Indian J. Pharmaceut. Sci. 68 (2006).
[24] V.B. Narayanswamy, M.M. Setty, S. Malini, A. Shirwaikar, Preliminary aphrodisiac activity of Hybanthus enneaspermus in rats, Pharmacologyonline 1 (2007) 152–161.
[25] M. Setty, V.B. Narayanaswamy, K.K. Sreenivasan, A. Shirwaikar, Free radical scavenging and nephroprotective activity of Hybanthus enneaspermus (L) F. Muell, Pharmacologyonline 2 (2007) 158–171.
[26] S. Tripathy, S. Parchuri, D. Pradhan, Preliminary investigation of the anti-inflammatory properties of Hybanthus enneaspermus, Int J Univ Pharm Life Sci. 1 (2011) 239–248.
[27] B. Pharmacopoeia, Department of Health and Social Security Scottish Home and Health Department, Office of the British Pharmacopoeia Commission, UK, 1988, p. 713, 2.
[28] J.F. Woessner Jr., The determination of hydroxyproline in tissue and protein samples containing small proportions of this imino acid, Arch. Biochem. Biophys. 93 (1961) 440–447, https://doi.org/10.1016/0003-9861(61)90291-0.
[29] O. Classics Lowry, N. Rosebrough, A. Farr, R. Randall, Protein measurement with the Folin phenol reagent, J. Biol. Chem. 193 (1951) 265–275.
[30] R.O. Datiashvili, J.H. Yueh, Management of complicated wounds of the extremities with scapular fascial free flaps, J. Reconstr. Microsurg. 28 (2012) 521–528, https://doi.org/10.1055/s-0032-1315772.
[31] B.S. Teo, R.Y. Gan, S. Abdul Aziz, T. Sirirak, M.F. Mohd Asmani, E. Yusuf, In vitro evaluation of antioxidant and antibacterial activities of Eucheuma cottonii extract and it's in vivo evaluation of the wound-healing activity in mice, J. Cosmet. Dermatol. 20 (2021) 993–1001, https://doi.org/10.1111/jocd.13624.
[32] O. Sarheed, A. Ahmed, D. Shouqair, J. Boateng, Wound Healing-New Insights into Ancient Challenges, InTech, Rijeka, Croatia, 2016.
[33] S.A. Guo, L.A. DiPietro, Factors affecting wound healing, J. Dent. Res. 89 (2010) 219–229, https://doi.org/10.1177/0022034509359125.
[34] M. Catauro, M.G. Raucci, F. De Gaetano, A. Marotta, Antibacterial and bioactive silver-containing Na 2 O· CaO· 2SiO 2 glass prepared by sol-gel method, J. Mater. Sci. Mater. Med. 15 (2004) 831–837.
[35] R. Cathrine, R. Ragunathan, K. Prasanna Kumar, Biosynthesis of silver nanoparticles using L. Acidophilus (probiotic bacteria) and its application, Int. J. Nanotechnol. Appl. 4 (2010) 217–222.
[36] J.M. Baron, M. Glatz, E. Proksch, Optimal support of wound healing: new Insights, Dermatology 236 (2020) 593–600, https://doi.org/10.1159/000505291.
[37] T. Leavitt, M.S. Hu, C.D. Marshall, L.A. Barnes, H.P. Lorenz, M.T. Longaker, Scarless wound healing: finding the right cells and signals, Cell Tissue Res. 365 (2016) 483–493, https://doi.org/10.1007/s00441-016-2424-8.
[38] A. Dehnoee, R.J. Kalbasi, M. Zangeneh, M.R. M.Delnavazi, A. Zangeneh, One-step synthesis of silver nanostructures using Heracleum persicum fruit extract, their cytotoxic activity, anti-cancer and anti-oxidant activities, Micro & Nano Lett. (2023) 11.
[39] A. Dehnoee, R. Javad Kalbasi, M.M. Zangeneh, et al., Characterization, anti-lung cancer activity, and cytotoxicity of bio-synthesized copper nanoparticles by Thymus fedtschenkoi leaf extract, J. Cluster Sci. 35 (2024) 863–874, https://doi.org/10.1007/s10876-023-02512-w.
[40] L. Ma, A. Ahmeda, K. Wang, A.R. Jalalvand, K. Sadrjavadi, M. Nowrozi, X. Wang, Introducing a novel chemotherapeutic drug formulated by iron nanoparticles for the clinical trial studies, Appl. Organomet. Chem. 36 (12) (2022) e5498, https://doi.org/10.1002/aoc.5498.
[41] H. Zhao, H. Su, A. Ahmeda, et al., Biosynthesis of copper nanoparticles using Allium eriophyllum Boiss leaf aqueous extract; characterization and analysis of their antimicrobial and cutaneous wound-healing potentials, Applied Organom Chemis 36 (2022) e5587.
[42] Muhammad Ishaq, Parham Taslimi, Zahid Shafiq, Samra Khan, Ramin Ekhteiari Salmas, Mohammad M. Zangeneh, Aamer Saeed, et al., Synthesis, bioactivity and binding energy calculations of novel 3-ethoxysalicylaldehyde based thiosemicarbazone derivatives, Bioorg. Chem. 100 (2020) 103924, https://doi.org/10.1016/j.bioorg.2020.103924. (Accessed 24 May 2024).
[43] J. Liu, A. Zangeneh, M.M. Zangeneh, B. Guo, Antioxidant, cytotoxicity, anti-human esophageal squamous cell carcinoma, anti-human Caucasian esophageal carcinoma, anti-adenocarcinoma of the gastroesophageal junction, and anti-distal esophageal adenocarcinoma properties of gold nanoparticles green synthesized by Rhus coriaria L. fruit aqueous extract, J. Exp. Nanosci. 15 (1) (2020) 202–216, https://doi.org/10.1080/17458080.2020.1766675.
[44] A. Ahmeda, M.M. Zangeneh, A. Zangeneh, Green formulation and chemical characterization of Lens culinaris seed aqueous extract conjugated gold nanoparticles for the treatment of acute myeloid leukemia in comparison to mitoxantrone in a leukemic mouse model, Appl. Organomet. Chem. 34 (3) (2020) e5369, https://doi.org/10.1002/aoc.5369.
[45] A. Ahmeda, A. Zangeneh, M.M. Zangeneh, Green synthesis and chemical characterization of gold nanoparticle synthesize using Camellia sinensis leaf aqueous extract for the treatment of acute myeloid leukemia in comparison to daunorubicin in a leukemic mouse model, Appl. Organomet. Chem. 34 (2020) e5290.
[46] A. Shedoeva, D. Leavesley, Z. Upton, C. Fan, Wound healing and the use of medicinal plants, Evid. base Compl. Alternative Med. 2019 (2019), https://doi.org/10.1155/2019/2684108.
[47] T. Kondo, Y. Ishida, Molecular pathology of wound healing, Forensic Sci. Int. 203 (2010) 93–98, https://doi.org/10.1016/j.forsciint.2010.07.004.
[48] T.J. Koh, L.A. DiPietro, Inflammation and wound healing: the role of the macrophage, Expet Rev. Mol. Med. 13 (2011) e23, https://doi.org/10.1017/S1462399411001943.
[49] A. Gragnani, B.R. Müller, I.D. Silva, S.M. Noronha, L.M. Ferreira, Keratinocyte growth factor, tumor necrosis factor-alpha and interleukin-1 beta gene expression in cultured fibroblasts and keratinocytes from burned patients, Acta Cir. Bras. 28 (2013) 551–558, https://doi.org/10.1590/S0102-86502013000800001.
[50] R.B. Diller, A.J. Tabor, The role of the extracellular matrix (ECM) in wound healing: a review, Biomimetics 7 (2022) 87, https://doi.org/10.3390/biomimetics7030087.
[51] N.X. Landén, D. Li, M. Ståhle, Transition from inflammation to proliferation: a critical step during wound healing, Cell. Mol. Life Sci. 73 (2016) 3861–3885, https://doi.org/10.1007/s00018-016-2268-0.
[52] R. Singla, S. Soni, V. Patial, P.M. Kulurkar, A. Kumari, S. Mahesh, Y.S. Padwad, S.K. Yadav, In vivo diabetic wound healing potential of nanobiocomposites containing bamboo cellulose nanocrystals impregnated with silver nanoparticles, Int. J. Biol. Macromol. 105 (2017) 45–55, https://doi.org/10.1016/j.ijbiomac.2017.06.109.
[53] S. Goswami, A. Kandhare, A.A. Zanwar, M.V. Hegde, S.L. Bodhankar, S. Shinde, S. Deshmukh, R. Kharat, Oral l-glutamine administration attenuated cutaneous wound healing in Wistar rats, Int. Wound J. 13 (2016) 116–124, https://doi.org/10.1111/iwj.12246.
[54] S.S. Mathew-Steiner, S. Roy, C.K. Sen, Collagen in wound healing, Bioengineering 8 (2021) 63, https://doi.org/10.3390/bioengineering8050063.
[55] V.Y. Barku, Wound healing current perspectives. IntechOpen; London, UK: Wound Healing: Contributions from Plant Secondary Metabolite Antioxidants, 2019.
[56] O.A. Ahmed, S.M. Badr-Eldin, M.K. Tawfik, T.A. Ahmed, M. Khalid, J.M. Badr, Design and optimization of self-nanoemulsifying delivery system to enhance quercetin hepatoprotective activity in paracetamol-induced hepatotoxicity, J. Pharmaceut. Sci. 103 (2014) 602–612, https://doi.org/10.1002/jps.23834.
[57] P. Roy, S. Amdekar, A. Kumar, R. Singh, P. Sharma, V. Singh, In vivo antioxidative property, antimicrobial and wound healing activity of flower extracts of Pyrostegia venusta (Ker Gawl) Miers, J. Ethnopharmacol. 140 (2012) 186–192, https://doi.org/10.1016/j.jep.2012.01.008.
[58] R. Świergosz-Kowalewska, A. Bednarska, A. Kafel, Glutathione levels and enzyme activity in the tissues of bank vole Clethrionomys glareolus chronically exposed to a mixture of metal contaminants, Chemosphere 65 (2006) 963–974, https://doi.org/10.1016/j.chemosphere.2006.03.040.

[59] J. Finaud, G. Lac, E. Filaire, Oxidative stress: relationship with exercise and training, Sports Med. 36 (2006) 327–358, https://doi.org/10.2165/00007256-200636040-00004.
[60] A.D. Kandhare, J. Alam, M.V. Patil, A. Sinha, S.L. Bodhankar, Wound healing potential of naringin ointment formulation via regulating the expression of inflammatory, apoptotic and growth mediators in experimental rats, Pharmaceut. Biol. 54 (2016) 419–432, https://doi.org/10.3109/13880209.2015.1038755.
[61] Z. Tessema, Y. Molla, Evaluation of the wound healing activity of the crude extract of root bark of Brucea antidysentrica, the leaves of Dodonaea angustifolia and Rhamnus prinoides in mice, Heliyon 7 (2021) e05901, https://doi.org/10.1016/j.heliyon.2021.e05901.